JOURNAL OF AGRICULTURAL AND FOOD CHEMISTRY

High-Throughput Quantitation of Peroxyl Radical Scavenging Capacity in Bulk Oils

KAI XIN HAY,[†] VIDURANGA YASHASVI WAISUNDARA,[†] MARK TIMMINS,[§] BOXIN OU,[#] KATHLEEN PAPPALARDO,[#] NANCY MCHALE,[#] AND DEJIAN HUANG*,[†]

Food Science and Technology Programme, Department of Chemistry, National University of Singapore, 3 Science Drive 3, Singapore 117543, Republic of Singapore; BD Biosciences, 2 Oak Park Drive, Bedford, Massachusetts 01730; and Brunswick Laboratories, 6 Thatcher Lane, Wareham, Massachusetts 02571

Autoxidation of methyl linoleate (8:2 mixture with decane, 37 °C) was induced by 2,2′-azobis(2,4-dimethylvaleronitrile) (AMVN, 17.7 mM) and the kinetics of oxygen consumption monitored using a 96-well microplate coated with an oxygen-sensitive fluorescence probe, a ruthenium dye, embedded in a silicone matrix at the bottom of the microplate. The probe does not participate in the reaction; instead, its fluorescence intensity is inversely proportional to the solution oxygen concentration as it changes during oxidation. In the absence of antioxidants, the oxidation rate has a linear relationship with the square root of the initiator concentrations. This is in agreement with theoretical autoxidation kinetics equations. In the presence of tocopherol-type antioxidants, a sharp lag phase appears. The quantitation of the antioxidant capacity is achieved using the area under the curve (AUC) approach. The assay has a 2 h running time, a linearity range from 1.56 to 18.7 μM (Trolox), and a limit of quantitation at 2.7 μM Trolox equivalency. The peroxyl radical scavenging capacities of several cold-pressed and organically grown plant seed oils were quantified along with the tocopherol concentrations of the oils. Tocopherols contribute only a fraction of the peroxyl radical scavenging capacity of the oils, and there is poor correlation between total tocopherol concentrations and radical scavenging capacity, suggesting that the antioxidant capacity of oils is due not only to tocopherols but also to other lipid-soluble antioxidants.

KEYWORDS: High-throughput; antioxidant; fluorescence; kinetics; seed oils; tocopherols

INTRODUCTION

The food industry has been taking advantage of the desirable features of partially hydrogenated vegetable oils for many decades. Produced from the incomplete catalytic hydrogenation of soy oil, partially hydrogenated oil renders cost-effectiveness, favorable physical properties for food processing, good taste to the product, and resistance to rancidity. As a result, foods prepared using partially hydrogenated oils enjoy much longer shelf life than their natural vegetable oil counterparts. However, the flipside of this seemingly wonderful oil is that it contains a large amount (~20%) of *trans* fatty acids (TFA), which are health hazards. Evidence has suggested that chronic consumption of TFA leads to cardiovascular diseases by decreasing high-density lipoprotein (HDL, the "good" cholesterol) and increasing the low-density lipoprotein (LDL, the "bad" cholesterol) (*1*, *2*). The Institute of Medicine of the United States, in its report on TFA, recommended that the tolerable upper intake level (UL) for TFA is zero (*3*). The U.S. Food and Drug Administration has accordingly declared that there is no healthy level of TFA in the diet and has demanded food companies to disclose TFA amounts on food labels starting this year (*4*). Consequently, the food companies have been searching for a healthy substitute for partially hydrogenated oil in developing TFA-free products.

One desirable property of TFA is resistance to autoxidation. On the contrary, the naturally occurring vegetable oils are prone to autoxidation due to their high content of polyunsaturated fatty acids (PUFA). Therefore, protection of the oils from autoxidation becomes an important issue in the selection of a replacement for the partially hydrogenated oils. The radical scavenging capacity is also a measure of the nutritional value of the oils, which contain lipid-soluble antioxidants such as tocopherols. Yet, there is lack of a high-throughput assay in quantifying the radical scavenging antioxidant capacity of oils that can be easily adapted in common food research laboratories to meet the high demand of the dietary antioxidant research related to lipids and fats. Applying a noninvasive molecular probe as an oxygen sensor, we report herein such a high-throughput assay. We coined this assay $ORAC_{oil}$, standing for oxygen radical absorbance capacity in bulk oil. Coupling an automatic liquid

* Author to whom correspondence should be addressed (e-mail chmhdj@nus.edu.sg).
[†] National University of Singapore.
[§] BD Biosciences.
[#] Brunswick Laboratories.

10.1021/jf061410v CCC: $33.50
Published on Web 06/29/2006

handling system with a microplate fluorescence reader, this assay can monitor the kinetics of 96 reactions simultaneously and measure many samples a day. The $ORAC_{oil}$ assay will not only help to assess the antioxidant nutrients in food lipids but also facilitate efforts to develop healthy and antioxidant-rich alternatives to partially hydrogenated oils.

EXPERIMENTAL PROCEDURES

Materials. Methyl linoleate (ML, 97%) was purchased from Tokyo Chemical Industry Co. Ltd. (Tokyo, Japan). Trolox (97%) was purchased from Aldrich Chemical Co. (Milwaukee, WI). α-Tocopherol was purchased from the United States Pharmacopoeia (Rockville, MD). Tocopherol-stripped corn oil was obtained from Dyet, Inc. (Bethlehem, PA). Cold-pressed seed oils were gifts from Rapunzel Pure Organics, Inc. (Valatie, NY). 2,2′-Azobis(2,4-dimethylvaleronitrile) (AMVN) was a gift from Wako Chemicals USA, Inc. (Richmond, VA). Tocotrienol samples were supplied from Davos Life Science Pte. Ltd. (Singapore). The oxygen biosensor system (OBS), a 96-well, round-bottom microplate coated with an oxygen-sensitive ruthenium dye, was purchased from BD Biosciences Discovery Labware (Bedford, MA). Solvents were of HPLC grade from commercial sources.

Instruments. A Synergy HT fluorescent microplate reader with an excitation wavelength of 485 nm and an emission wavelength of 630 nm (Bio-tek Instruments Inc., Winooski, VT) was used to monitor the autoxidation reaction in OBS. Sample dilutions and reaction solution mixtures were performed manually or by the Precision 2000 automatic liquid handling systems (Bio-tek Instruments Inc.). The tocopherol profiles of seed oils were analyzed on an ESA high-performance liquid chromatography (HPLC) system with a Coularray eight-channel detector (ESA, Inc., Chelmsford, MA). Separation was accomplished on a Zorbax C18 column (Hewlett-Packard, Palo Alto, CA) (2.1 mm, 150 mm, 3 μm, column temperature of 37 °C) at 37 °C with a mobile phase of 70% methanol at a flow rate of 0.3 mL/min, and the UV detector was set at 280 nm.

$ORAC_{oil}$ Assay Method. A ML and decane mixture (8:2 v/v, 150 μL) was pipetted to the 96-well OBS plate and mixed with samples or Trolox standard solutions (25 μL). Typically the standard solutions were tested in duplicate to the fixed well positions in each run to facilitate data processing. The perimeter wells were filled with ML (150 μL) and blank [25 μL of ML/decane (8:2)]. Samples were dissolved and diluted to proper concentrations using the ML/decane mixture (8:2). Each sample was run in triplicate, and some of them were tested with five different concentrations to ensure dose response versus the net area under the curve (AUC) was maintained. The mixtures of sample and ML (175 μL) were incubated for 10 min at 37 °C prior to addition of AMVN (25 μL, 17.6 mg/mL in ML/decane (8:2)mixture). The OBS plate was then sealed with plastic tape, and the kinetics of the oxygen consumption was monitored for 2 h at 37 °C with one fluorescence reading taken every minute from the bottom of the plate. The plate was shaken with low intensity for 5 s before each reading to ensure sufficient mixing. The fluorescence data were converted to a normalized oxygen concentration following a published procedure (*11*). As the reactions proceed, oxygen in the wells is depleted and the fluorescence reading reaches its maximum. The rate of decrease of the oxygen concentration is taken as a measure of the oxygen consumption rate (*5*). The fluorescence reading was transformed to oxygen concentration according to the Stern−Volmer equation

$$I_0/I = 1 + K_{SV}[O_2]$$

where I_0 is the fluorescence intensity in the absence of oxygen, I is the fluorescence intensity in the presence of oxygen at concentration $[O_2]$, and K_{SV} is the Stern−Volmer constant (*6*). The oxygen concentration was normalized to the initial, ambient concentration. AUC of oxygen concentration plot over time is used to calculate the radical scavenging capacity. The AUC approach has been successfully applied in antioxidant capacity assays (*7*). Independent knowledge of the solubility of oxygen in the reaction mixture would be required to obtain absolute oxygen concentrations. Herein, absolute oxygen concentration is not essential. Nonetheless, the ML/decane solution was sufficiently agitated to ensure air saturation.

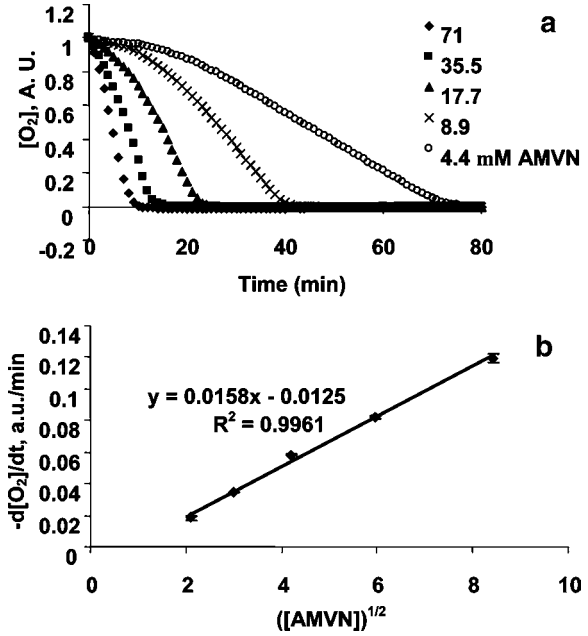

Figure 1. (**a**) Autoxidation of ML (TCI) in the absence of added antioxidants under different concentrations of AMVN. As the AMVN concentration decreases, a lag phase appears, indicating there are residual antioxidants in the ML. (**b**) Plot of oxygen consumption rate and square root of AMVN concentrations ($n = 3$).

RESULTS

ML autoxidation in an air-saturated solution was initiated by the lipid-soluble azo radical initiator AMVN. The reaction was carried out in closed wells in an OBS microplate sealed with transparent plastic tape. As the reaction proceeds, oxygen in the well is consumed, and the fluorescence reading reaches the maximum when the oxygen is depleted. The reaction rate is dependent on the radical initiator concentrations. To determine an appropriate AMVN concentration for use in subsequent experiments, oxygen consumption was monitored at various concentrations of AMVN in the absence of antioxidants. The results of this experiment are shown in **Figure 1**, where relative oxygen concentration (normalized to the ambient starting condition) is plotted.

It can be seen from **Figure 1a** that the relative oxygen consumption rate R_{un} decreases with decreasing AMVN concentration and that at lower AMVN concentrations a lag phase appears during which the $[O_2]$ remains at ambient for a while before decreasing. We attribute this to residual antioxidants present in the ML, as corroborated by data to be shown below, which shows that added inhibitor can prolong this lag phase. In fact, high-performance liquid chromatography of the pure ML from TCI or Aldrich shows a number of impurities that absorb light around 250 nm, indicating possible aromatic impurities (data not shown). The high concentration of ML (2.4 M) used here also increases the concentration of the impurity in the assay solution, thus making it possible to observe the lag phase for blank run at low radical initiator concentration. At higher concentrations of AMVN, the radical flux rate is large enough that this amount of antioxidant may be too low to cause a measurable induction period. Nonetheless, the plot of the oxygen consumption rates (obtained from the uninhibited stage

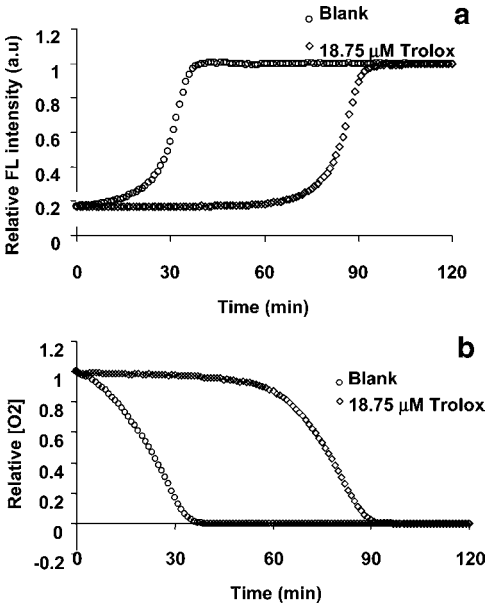

Figure 2. Kinetic curves of ML oxidation initiated by AMVN (17.7 mM) at 37 °C. Circles represent uninhibited reaction, and diamonds refer to 18.75 μM Trolox. The oxygen consumption kinetic curve is obtained from mathematical transformation of the fluorescence reading by the equation $[O_2] = (I_0/I - 1)/(DR - 1)$. DR is dynamic range and is equivalent to the ratio between the last FL reading when O_2 is depleted and the first reading when O_2 in the solution is saturated.

of the reactions) and the square root of AMVN concentrations gives a linear curve, and this demonstrates that the reaction obeys basic uninhibited autoxidation kinetics (vide infra). The small lag phase that appeared in the uninhibited blank does not affect subsequent assay results because the AUC of the blank is subtracted. In our earlier work, we have demonstrated that radical initiator (AAPH) concentrations did not affect the antioxidant capacity values in the $ORAC_{FL}$ assay (*8*). In this assay we chose the final concentration of AMVN to be 17.7 mM so that the assay can be finished within a reasonable time and with sufficient sensitivity.

Using the 96-well OBS microplate, multiple samples could be tested simultaneously using the format of sample layout with standards tested in duplicates and samples tested in triplicates. The quantitation was accomplished using the AUC approach similar to what is used in the $ORAC_{FL}$ assay (*7*). The AUC is obtained from the oxygen concentration change curves (**Figure 2**).

The AUC is calculated according to the oxygen concentration versus time plot (*n* is the number of the last reading and *t* is the time interval between readings)

$$AUC = [0.5([O_2]_0 + [O_2]_n) + [O_2]_0 + [O_2]_1 \ldots + [O_2]_i + \ldots [O_2]_n]t$$

where $[O_2]_i$ represents the normalized oxygen concentration at *i* min of the reaction and *t* is the time interval between readings. For the curves shown in **Figure 2**, the AUC for blank is calculated to be 22.5 and the AUC for 18.75 μM Trolox is 46.9. Thus, the net AUC is 24.4 (au·min). The AUC is a multiplication of time and concentration of oxygen at a given time; thus, it combines the inhibition time and degree of a given antioxidant. A typical standard curve is shown in **Figure 3**.

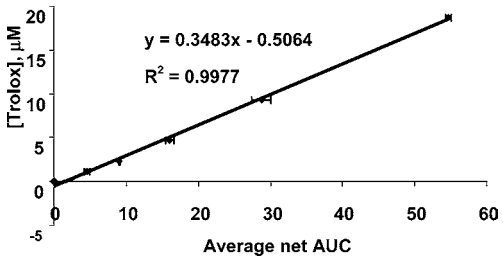

Figure 3. Typical standard curve of $ORAC_{oil}$ assay ($n = 3$).

The linearity ranges from 1.56 to 18.7 μM. The average blank AUC ($n = 12$) is 22.5 ± 0.7, and the corresponding limit of detection (LOD, 3σ) is 24.7 au·min or 0.70 μMTE and the limit of quantitation (LOD, 10σ) is 29.7 au·min or 2.66 μMTE. The $ORAC_{oil}$ value of a sample is calculated using the standard curve as follows:

$$ORAC_{oil} = \frac{\text{slope} \times (\text{net auc of sample}) + \text{intercept}}{[\text{sample}]}$$

The unit of the $ORAC_{oil}$ value is dependent on the concentration used. Typically, for solid samples, the concentration is expressed as micromoles of TE per gram, and for liquid samples the concentration is micromoles of TE per liter. For pure compounds, molar concentration is conveniently used for better comparison. The average of the 10 day data of α-tocopherol (1.06 ± 0.07 TE) gave a relative standard deviation (RSD) of <10%. To correct any variations caused by initiator concentrations, microplate, and temperature fluctuation, it is recommended to run the standards with five different concentrations in duplicates simultaneously with the sample. The averaged standard curve of each run is used to calculate the ORAC values of the samples in the same plate. It is also important that the Trolox working solution be made fresh daily as it is sensitive to oxidation over extended storage at room temperature or in a refrigerator.

Using this new method, we determined the antioxidant capacities of organic cold-pressed seed oils. These values as well as the tocopherol profiles determined by HPLC are listed in **Table 1**. From the data, it is apparent that except for pumpkin oils, $ORAC_{oil}$ values are typically higher than tocopherol concentrations. Moreover, there is no linear correlation between total tocopherol contents and antioxidant capacity (**Figure 4**). Apparently, lipid-soluble antioxidants other than tocopherols significantly contribute to antioxidant capacity. This is especially the case for cold-pressed olive oils.

The dose−responses of selected samples gave good linearity as shown in **Figure 5**. The high-throughput fashion allows for parallel measurements of 15 samples in triplicates per OBS microplate.

DISCUSSION

Assay Principle. Unassisted lipid autoxidation is rather slow and not efficient for the purpose of measuring antioxidant activity at room temperature. Therefore, in an experimental assay protocol, it is common practice to apply heat or radical initiators to accelerate the oxidation progress (*9*). Commonly used initiators are azo compounds and transition metal ions [Fe(II), Cu(II)] (*10*). The oxidation substrates are normally polyunsaturated fatty acid esters that bear chemical similarity to vegetable oils. However, naturally occurring vegetable oils are not the ideal substrates for quantitative assays because of lot-to-lot

Table 1. $ORAC_{oil}$ Values and Tocopherol Contents of Edible Oils ($n = 3$)[a]

seed oil	$ORAC_{oil}$ (μmol of TE/L)	α-T (μM)	β-T (μM)	γ-T (μM)	δ-T (μM)	β-TT (μM)	total tocopherols (μM)
stripped corn oil	332 ± 14			17			17
avocado	580 ± 54	158					158
hazelnut	2521 ± 357	630					630
sunflower	2532 ± 286	1276					1277
pumpkin	2542 ± 399	158		1060	156	1594	2969
canola	2766 ± 315	481					481
sesame	2805 ± 364			608			608
safflower	3094 ± 363	1220					1221
olive	3153 ± 205	313					314
soy	4383 ± 235	160	245.1	1956	865.3		3228

[a] T, tocopherol; TT, tocotrienol. Blank field indicates no detectable amount of the tocopherols was found in the oil.

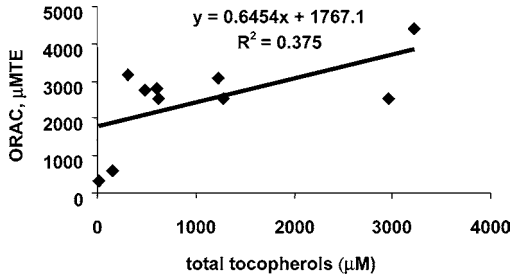

Figure 4. Correlation of ORAC values and total tocopherol concentrations in cold-pressed seed oils.

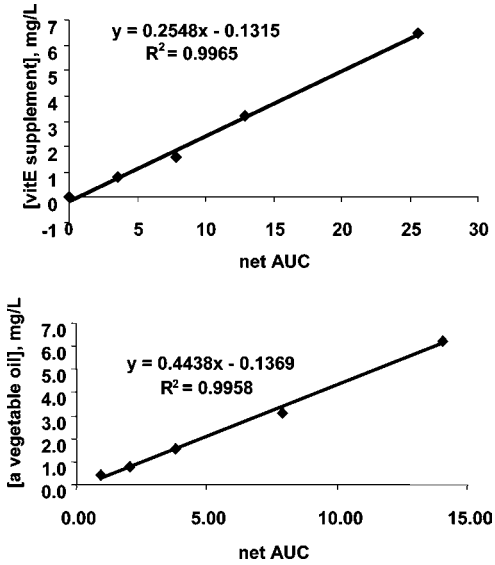

Figure 5. Linear relationships of commercial samples versus area under the curve.

variability intrinsic to the products, which are mixtures of unsaturated fatty acid triglycerides. Therefore, we have selected methyl linoleate as the substrate to avoid potential variability and to simplify quality control. When ML reacts with oxygen initiated by a radical, lipid peroxides are formed as primary oxidation products, which may further decompose to hexanal as a secondary oxidation product. Radical scavenging antioxidants can effectively inhibit the radical chain reaction (*11*).

In the autoxidation of ML induced by AMVN, the oxygen consumption rate was obtained from the following scheme of elementary reactions (LH = methyl linoleate, R_2N_2 = AMVN).

initiation

$$R_2N_2 \rightarrow 2R^\bullet + N_2 \quad (1)$$

$$R^\bullet + O_2 \rightarrow ROO^\bullet \quad (2)$$

$$ROO^\bullet + LH \rightarrow ROOH + L^\bullet \quad (3)$$

propagation

$$L^\bullet + O_2 \rightarrow LOO^\bullet \quad (4)$$

$$LOO^\bullet + LH \rightarrow LOOH + L^\bullet \quad (5)$$

inhibition and termination

$$LOO^\bullet + AH \rightarrow LOOH + A^\bullet \quad (6)$$

$$A^\bullet + LOO^\bullet \rightarrow \text{non-radical products} \quad (7)$$

$$LOO^\bullet + LOO^\bullet \rightarrow \text{non-radical products} \quad (8)$$

Under steady-state approximation, the rates of uninhibited (R_{un}) and inhibited (R_{inh}) oxygen consumption can be expressed by the following equations (*12*):

$$R_{un} = \{k_3/(2k_8)^{1/2}\}[LH]R_i^{1/2} \quad (9)$$

$$R_{inh} = \{k_3[LH]R_i\}/\{nk_6[AH]\} \quad (10)$$

Equation 10 was derived by assuming that all generated peroxyl radicals $ROO^\bullet$ initiate new propagation chains and that AH reacts with only $LOO^\bullet$. According to this kinetic model, the initial inhibited reaction rate R_{inh} is inversely proportional to the initial antioxidant concentration [AH]. Taking advantage of eq 10 Ingold (*11*), Pryor (*14*), and Niki (*13*) have calculated k_{inh} (k_6 here) between $LOO^\bullet$ and AH in micelles and liposomal membranes. The data obtained from this assay in bulk oil show that R_{inh} is independent of [AH] as demonstrated in **Figure 2**. Instead, the oxygen concentration change is insignificant in the lag phase. In bulk oil and in the presence of a radical initiator, R_2N_2, the competitive reaction between $ROO^\bullet$ and AH or LH (eqa 11 and 12) may be significant and alter the kinetic equation:

$$ROO^\bullet + AH \rightarrow ROOH + A^\bullet \quad (11)$$

$$ROO^\bullet + A^\bullet \rightarrow ROOA \quad (12)$$

For vitamin E, the reaction rate constants of k_{11} and k_6 should be comparable at $\sim 2.0 \times 10^6$ M^{-1} s^{-1}. Likewise, k_3 and k_5 are

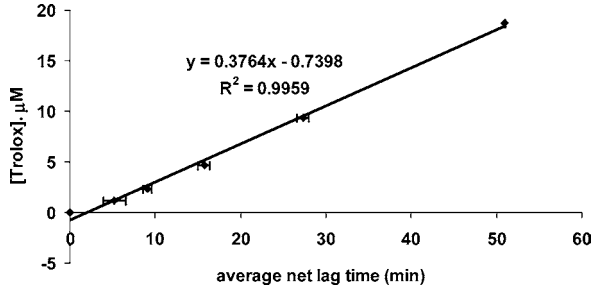

Figure 6. Standard curve of the Trolox concentration versus net lag time plot ($n = 3$).

much lower at ~60 M^{-1} s^{-1} (*13*). This difference of >4 orders of magnitude in rates makes it possible that generated ROO• is solely trapped by AH and its concentration is high. In this case the oxygen consumption rate would be equal to the rate of radical initiation and not dependent on the antioxidant concentrations. Esterbauer and Abuja simulated the kinetics of low-density lipoprotein oxidation inhibited by α-tocopherol, and the results indeed showed that LOOH formation is only slightly enhanced with increasing concentrations of tocopherol (*14*). As the reaction proceeds, oxygen concentration gradually increases, indicating increasing significance of reaction between ROO• and ML. Eventually, transition to uninhibited reaction occurs and the oxygen depletion is rapid until all of the dissolved oxygen is consumed. In the absence of oxygen, the oxidation reaction stops but radical (R•) is still generated through thermal decomposition of AMVN.

Quantitation of Antioxidant Capacity. For a discrete chemical compound, the antioxidant property can be described by the rate constant of reaction 6 k_6 (or k_{inh}) and the number (n) of radicals one antioxidant molecule can scavenge (or stoichiometric factor). According to eq 10, the plot of R_{inh} versus $[AH]^{-1}$ would give a straight line with a slope of $k_3[LH]R_i/nk_6$. Pryor and co-workers calculated the k_6 values of a series of antioxidants by comparing slopes of the sample with that of α-tocopherol (*16*). However, when R_{inh} is not sensitive to the antioxidant concentration, as is the case here, it is not possible to generate a meaningful plot for the calculation of k_6. The stoichiometric factor, n, was obtained from the plot of antioxidant concentration versus lag time. The relationship of the lag time of a typical antioxidant and its concentration is expressed as (*15*, *16*)

$$t_{inh} = n[AH]/R_i \quad (13)$$

where n is the number of radicals the antioxidant can scavenge and t_{inh} is the lag time. The slope of the lag time versus the antioxidant concentration plot is n/R_i. With a known R_i, n can be calculated. Alternatively, comparing the slope of the sample with that of a standard antioxidant (i.e., α-tocopherol) with $n = 2$, the antioxidant capacity of the sample can be obtained from two slopes (*16*). The kinetic curves obtained using the $ORAC_{oil}$ assay show a sharp transition from inhibited to uninhibited reaction, and consequently the lag time was obtained with certainty (*15*). First, a line was drawn to the inhibited oxidation curve at the early stage of the reaction. Its intersection with the straight lines drawn through the points taken in the uninhibited reaction gives the lag time.

The small lag time from the blank was subtracted to give net lag time. Indeed, linear regression fit of the data of lag time versus the concentrations of Trolox (**Figure 6**) gives a straight line with excellent regression coefficiency ($R^2 > 0.99$) and

Table 2. $ORAC_{oil}$ Values of Commercial Tocopherol and Tocotrienol Samples ($n = 3$)

sample ID	$ORAC_{oil}$ by AUC (μmol of TE/L)	$ORAC_{oil}$ by lag time (μmol of TE/L)	ratio
1	1783 ± 34	1621 ± 8	0.91
2	2104 ± 127	2161 ± 90	1.02
3	2735 ± 318	2424 ± 191	0.89
4	2943 ± 205	2587 ± 162	0.88
5	1895 ± 254	1621 ± 247	0.86
6	3123 ± 295	3483 ± 405	1.11
7	1493 ± 115	1837 ± 73	1.23
8	1738 ± 233	1565 ± 228	0.90
9	1814 ± 175	1605 ± 221	0.88
10	1700 ± 141	1609 ± 75	0.95

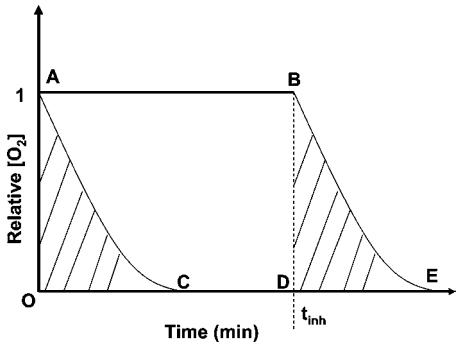

Figure 7. Relationship between net AUC and lag time in a hypothetical inhibited autoxidation (close similarity to **Figure 6**). The net AUC of an inhibited reaction equals the area of ACEB minus the shaded area of OAC, which is the same as the area of BDE. Thus, the net AUC is equivalent to the area of OABD, which equals t_{inh}. In reality, the net AUC and t_{inh} can be different if the inhibited phase has significant oxygen consumption leading to line AB being not parallel to the x-axis and obscuring the transition to uninhibited reaction.

negligible intercept. Thus, the antioxidant capacity of a sample was obtained according to the linear equation

$$ORAC_{oil}\ value = \frac{slope \times (net\ lag\ time) + intercept}{[sample]}$$

$ORAC_{oil}$ values of a group of commercial tocotrienol samples are thus obtained and listed in **Table 2** along with the $ORAC_{oil}$ values calculated using the AUC approach. The ratio of the two falls between 0.85 and 1.24. Taking into account a CV of ≈15% of the method, we can reasonably conclude that, for an antioxidant that gives a sharp reaction phase transition, the AUC and lag time approach to calculating $ORAC_{oil}$ values does not make a significant difference.

The relationship between net AUC and lag time is more apparent if we examine ideal kinetic curves of uninhibited and inhibited autoxidation. In an idealized inhibited autoxidation reaction where the oxygen consumption is negligible during the inhibition phase (illustrated in **Figure 7**), the net area under the curve has the same numerical values as the lag time but different units (AU·min vs min). The $ORAC_{oil}$ value in this ideal case reflects the sample's capacity sample in scavenging amount of peroxyl radicals (similar to the stoichiometric factor n) per unit weight or volume of the sample. Experimentally, they may be different due to non-negligible consumption of oxygen in the inhibited phase. If oxygen consumption is significant enough, the phase transition becomes obscured (*17*). This happens for less potent (smaller k_6 values) antioxidants

and lag time cannot be accurately obtained from the kinetic curves (*15*, *18*). The area under the curve approach thus overcomes this limitation and is more generally applicable to both situations for more accurate antioxidant capacity quantitation (*19*). In this case, the chemical meaning of the $ORAC_{oil}$ value is more complex. Kinetic simulations are needed to further decompose the contribution from the inhibition rate constant (k_6) and the number of radicals a sample can scavenge. For real-world food mixtures such as vegetable oils, antioxidant capacity is a more realistic and straightforward metric than kinetic rate constants, which are harder to define as potential synergistic and antagonistic interactions among different compounds present in the sample (*20*).

Several methods have been used in measuring the peroxyl radical scavenging activity of antioxidants, and a recent review summarizes the chemical principles of these methods (*21*). The kinetics of lipid peroxidation and inhibition has been monitored by conjugated diene peroxide concentration at 234 nm. Antioxidants typically absorb at the same wavelength and thus interfere. Quantitation of diene peroxide concentration using HPLC or colorimetric method is also rather time-consuming and labor-intensive. Alternatively, the oxygen consumption rate has been measured by Clark O_2 electrode if the reaction was carried out in water but not in oil as the membrane of the electrode is not oil compatible. For bulk oil assays, a pressure transducer under a pure oxygen atmosphere was applied, but this requires the experiment to be carried out in a pure oxygen atmosphere instead of air (*22*). Using a glass capillary microvolumometer under air atmosphere (*23*), Roginsky and coworkers studied the *p*-hydroquinones (QH_2) antioxidant activity by monitoring the oxygen consumption rates of AMVN-initiated oxidation of styrene. From the kinetic curves of oxygen consumption, the rate constant (k_6) of the reaction $ROO^{\bullet}$ with QH_2 and stoichiometric factor, *n*, were calculated for *p*-hydroquinones. These methods receive only limited attention due to the lack of commercially available experimental apparatus necessary to carry out a method validation in a different laboratory. The method reported herein directly monitors the oxygen concentrations in a normal atmospheric pressure and temperature in a high-throughput fashion. The $ORAC_{oil}$ assay provides a convenient and assessable tool for rapid screening of lipid-soluble antioxidants with commercially available OBS microplates and necessary chemical reagents. Thus, it can be readily adapted in typical food chemistry laboratories equipped with a microplate fluorescence reader.

In summary, a noninvasive approach for monitoring antioxidant capacity is proposed herein using oxygen probe coated microplates. With excellent reproducibility and sensitivity, the method can be used to quantify the antioxidant capacity of vegetable oils. It has been common practice to strip phenolic antioxidants present in vegetable oil to reduce their negative effect on the flavor and color of the oil. In light of the health benefits of antioxidants, it might be worthwhile to reconsider the current practice of refining in order to preserve the nutritional values of edible oils. With this assay, we are in a position to study the antioxidant capacity of pure compounds and botanical extracts in different reaction media including water, emulsion, and bulk oil systems. The $ORAC_{oil}$ assay complements the $ORAC_{FL}$ assay as it can handle highly lipophilic samples such as essential oils, food lipids, and plasma lipid extracts, which are hard to dissolve in water phase even with the help of cyclodextrin derivatives as solubility enhancers.

ACKNOWLEDGMENT

We appreciate the critical comments of Professor Vitaly Roginsky at N. N. Semenov Institute of Chemical Physics, Russian Academy of Sciences.

LITERATURE CITED

(1) Steen, S.; Joern, D. Influence of *trans* fatty acids on health. *Ann. Nutr. Metab.* **2004**, *48* (2), 61−66.
(2) Severson, K.; Warner, M. Fat substitute, once praised, is pushed out of the kitchen. *New York Times* **2005**, Feb 13.
(3) Panel on Macronutrients, Subcommittees on Upper Reference Levels of Nutrients and on Interpretation and Uses of Dietary Reference Intakes, and the Standing Committee on the Scientific Evaluation of Dietary Reference Intakes. *Dietary Reference Intakes for Energy, Carbohydrate, Fiber, Fat, Fatty Acids, Cholesterol, Protein, and Amino Acids*; Institute of Medicine: Washington, DC, 2002.
(4) *Fed. Regist.* **2004**, *69* (75, April 19).
(5) Dike, L. E.; Xia, H.; Guarino, R. D.; Presnell, S. C.; Timmins, M. R. Rapid method for assessing oxygen consumption rate of cells from transient-state measurements of pericellular dissolved oxygen concentration. *Cytotechnology* **2006**, in press.
(6) Stitt, D. T.; Nagar, M. S.; Haq, T. A.; Timmins, M. R Determination of growth rate of microorganisms in broth from oxygen-sensitive fluorescence plate reader measurements. *BioTechniques* **2002**, *32* (3), 684, 686, 688−689.
(7) Cao, G.; Alessio, H. M.; Culter, R. Oxygen-radical absorbance capacity assay for antioxidants. *Free Radical Biol. Med.* **1993**, *14*, 303−311.
(8) Prior, R. L.; Hoang, H.; Gu, L.; Wu, X.; Bacchiocca, M.; Howard, L.; Hampsch-Woodill, M.; Huang, D.; Ou, B.; Jacob, R. Assays for hydrophilic and lipophilic antioxidant capacity (oxygen radical absorbance capacity ($ORAC_{FL}$)) of plasma and other biological and food samples. *J. Agric. Food Chem.* **2003**, *51*, 3273−3279.
(9) Alessi, M.; Paul, T.; Scaiano, J. C.; Ingold, K. U. The contrasting kinetics of peroxidation of vitamin E-containing phospholipid unilamellar vesicles and human low-density lipoprotein. *J. Am. Chem. Soc.* **2002**, *124*, 6957−6965.
(10) Frankel, E. N.; Bosanek, C. A.; Meyer, A. S.; Silliman, K.; Kirk, L. L. Commercial grape juices inhibit the in vitro oxidation of human low-density lipoproteins. *J. Agric. Food Chem.* **1998**, *46*, 834−838.
(11) Davalos, A.; Bartolome, B.; Gomez-Cordoves, C. Inhibition of methyl linoleate autoxidation by phenolics and other related compounds under mild oxidative conditions**.** *J. Sci. Food Agric.* **2004**, *84* (7), 631−638.
(12) Barclay, L. R. C.; Ingold, K. U. Autoxidation of biological molecules. 2. Autoxidation of a model membrane. Comparison of the autoxidation of egg lecithin phosphatidylcholine in water and in chlorobenzene. *J. Am. Chem. Soc.* **1981**, *103*, 6478−6485.
(13) Niki, R.; Takahashi, M.; Komuro, E. Antioxidant activity of vitamin E in liposomal membranes. *Chem. Lett.* **1986**, 1573−1576.
(14) Abuja, P. M.; Esterbauer, H. Simulation of lipid peroxidation in low-density lipoprotein by a basic "skeleton" of reactions. *Chem. Res. Toxicol.* **1995**, *8*, 753−763.
(15) Boozer, C. E.; Hammond, G. S.; Hamilton, C. E.; Sen, J. N. Air oxidation of hydrocarbons. II. The stoichiometry and fate of inhibitors in benzene and chlorobenzene. *J. Am. Chem. Soc.* **1955**, *77*, 3233−3237.
(16) Pryor, W. A.; Cornicelli, J. A.; Devall, L. J.; Tait, B.; Trivedi, B. K.; Witiak, D. T.; Wu, M. A rapid screening test to determine the antioxidant potencies of natural and synthetic antioxidants. *J. Org. Chem.* **1993**, *58*, 3521−3532.
(17) Mahoney, L. M. Antioxidants. *Angew. Chem., Int. Ed. I* **1969**, *8*, 547−555.

(18) Huang, D.; Ou, B.; Hampsch-Woodill, M.; Flanagan, J. A.; Prior, R. L. High throughput assay of oxygen radical absorbance capacity (ORAC) using a multi-channel liquid handling system coupled with a microplate fluorescence reader in 96-well format. *J. Agric. Food Chem.* **2002**, *50*, 4437−4444.

(19) Cao, G.; Alessio, H. M.; Cutler, R. G. Oxygen-radical absorbance capacity assay for antioxidants. *Free Radical Biol. Med.* **1993**, *14* (3), 303−311.

(20) Niki, E.; Noguchi, N. Evaluation of antioxidant capacity. What capacity is being measured by which method? *IUBMB Life* **2000**, *50*, 323−329.

(21) Huang, D.; Ou, B.; Prior, R. Chemistry behind antioxidant capacity assays. *J. Agri. Food Chem.* **2005**, *53*, 1841−1856.

(22) Burton, G. W.; Ingold, K. U. Autoxidation of biological molecules. 1. The autoxidation of vitamin E and related chain-breaking antioxidants *in vitro*. *J. Am. Chem. Soc.* **1981**, *103*, 6472−6477.

(23) Loshadkin, D.; Roginsky, V.; Pliss, E. Substituted *p*-hydroquinones as a chain-breaking antioxidant during the oxidation of styrene. *Int. J. Chem. Kinet.* **2002**, *34*, 162−171.

Received for review May 18, 2006. Accepted May 24, 2006. D.H. thanks the National University of Singapore for funding of this project.

JF061410V